The tube wall of Cambrian anabaritids

ARTEM KOUCHINSKY and STEFAN BENGTSON

Kouchinsky, A. and Bengtson, S. 2002. The tube wall of Cambrian anabaritids. *Acta Palaeontologica Polonica* 47 (3): 431–444.

Celestite/barite-replaced and phosphate-replicated tubes of Early Cambrian anabaritids from the northern part of the Siberian Platform (Anabar Shield) give new evidence on the wall-structure of these enigmatic fossils. The walls consist of fibres, interpreted as reflecting an original aragonitic fabric. Bundles of fibres are arranged in growth lamellae, and the latter form an angle of at least 45° with the inner tube wall. Where the outer tube surface projects into annular flanges, the lamellae have a chevron-like section due to the backwards deflection of the outer parts. Anabaritids are usually referred to the Cnidaria or left without systematic assignment, but earlier suggestions included affinity to the serpulid polychaetes. The chevron structure resembles that previously exclusively known from serpulids, but the presence of internal tooth-like structures in anabaritid tubes, perhaps compromising up-and-down movement through the tubes, continue to make a direct assignment to the Serpulida questionable.

Key words: Anabaritida, biomineralization, wall structure, aragonite, celestite, barite, Cambrian, Siberia.

Artem Kouchinsky [artem.kouchinsky@geo.uu.se], Department of Earth Sciences, Historical Geology and Palaeontology, Norbyvägen 22, SE-752 36, Uppsala, Sweden; present adress: Department of Earth & Space Sciences, University of California L.A., Los Angeles, CA 90024, USA;
Stefan Bengtson [stefan.bengtson@nrm.se], Department of Palaeozoology, Swedish Museum of Natural History, Box 50007, SE-104 05, Stockholm, Sweden.

Introduction

Anabaritids were among the first animal groups to acquire a mineralized skeleton. Their triradially symmetrical, calcareous tubes are characteristic components of microfossil assemblages in Early Cambrian beds. They first appeared in the Manykayan (= Nemakit-Daldynian), i.e., pre-Tommotian as recognized on the Siberian Platform, and survived until the late Atdabanian or early Botomian, in the late Early Cambrian (Rozanov et al. 1969; Val'kov and Sysoev 1970; Val'kov 1982; Conway Morris and Chen 1989; Bengtson et al. 1990; Towe et al. 1992). Their distribution (summarized by Conway Morris and Chen 1989; and Missarzhevskij 1989) was worldwide.

The systematic affinity of anabaritids is controversial. Except for a few early suggestions that they represent tubicolous polychaetes (Voronova and Missarzhevskij 1969; Glaessner 1976), they have either been interpreted as cnidarians (Missarzhevskij 1974; Val'kov 1982; Fedonkin 1986, 1987; Kouchinsky et al. 1999) or as being of uncertain systematic affinity (Val'kov and Sysoev 1970; Matthews and Missarzhevsky 1975; Abaimova 1978; Conway Morris and Chen 1989; Missarzhevskij 1989; Bengtson et al. 1990; Towe et al. 1992). The uncertainty is mainly due to lack of data on anabaritid anatomy, including the structure and composition of their tube wall.

Information on the construction of the skeleton may help to elucidate anabaritid biology and relationships. A wider significance of such data on the early animal skeletons is that they yield insight into the evolution of biologically controlled mineralization. Whereas biologically induced mineralization is probably as old as life itself, the ability to control biominerals for tissue construction did not become widespread until the late Neoproterozoic and Cambrian (e.g., Lowenstam and Weiner 1989; Bengtson 1994). The Cambrian explosion of multicellular life was coincident with a burgeoning of skeletons. These were of various construction and composition; in all probability they arose independently in a number of different lineages. In view of the sophisticated biochemical controls necessary to nucleate and shape biominerals, however, there may well be underlying homologous mechanisms behind the evolution of mineralized skeletons (e.g., Lowenstam and Margulis 1980; Kirschvink and Hagadorn 2000). Comparing the constructional and mineralogical features of the earliest skeletons in the various lineages may reveal such homologies and, in addition, point to unrecognized homologies of skeletal tissues themselves.

As pointed out by Missarzhevsky (1974: 185), the presence of inwards directed spines in some anabaritids shows that at least those soft parts adjacent to the interior wall were firmly attached to the inner surface of the tube, rather than being able to slide up and down. Abaimova (1978) described extensive external keels in several taxa, sometimes wider than the diameter of the tube. She argued (p. 82) that these could only have been formed from the outside, and that therefore the anabaritid tube was to be considered an internal, supporting skeleton. Conway Morris and Bengtson (in Bengtson et al. 1990: 197) proposed, however, that the secreting tissue only covered the leading edges of the flanges.

The original wall of anabaritids has been interpreted to be aragonitic (Conway Morris and Chen 1989): a fibrous structure is sometimes visible on internal moulds, and when the shell is preserved in calcium carbonate it seems invariably recrystallized, with fine structures obliterated. What we know about the wall structure so far derives from phosphatized samples (Conway Morris and Chen 1989; Bengtson et al. 1990). Diagenetic calcium phosphate has a great potential for preserving delicate structures; however, with regard to skeletal elements it tends to preserve surfaces better than internal structures (Lucas and Prévôt 1991). Thus, satisfactory replication of shell surfaces can be achieved, either in positive or negative relief, during phosphatization (e.g., Runnegar 1985; Bengtson et al. 1990), but there are few examples of the three-dimensional fine structures of aragonitic fossil shells being preserved in phosphate. Conway Morris and Chen (1989) documented a fibrous inner layer with distinct spherulitic structure in phosphatized anabaritid tubes from China; the structure of the wall external to the spherulitic layer was considerably less clear, but was interpreted to consist of fine concentric laminae with a transverse fibrous fine structure. Phosphatized Australian anabaritids described by Conway Morris and Bengtson (in Bengtson et al. 1990) revealed only obscure traces of possible fibrous structure.

We have investigated new material of anabaritids from the northern Siberian Platform. In addition to phosphatized specimens, there are tubes preserved in celestite (strontium sulphate, $SrSO_4$) admixed with barite (barium sulphate, $BaSO_4$), which through partial replication of the original structure give the first direct evidence on the nature of the tube wall throughout its thickness. These new data serve to elucidate the relationship between the mineralized tubes and the soft tissues secreting them.

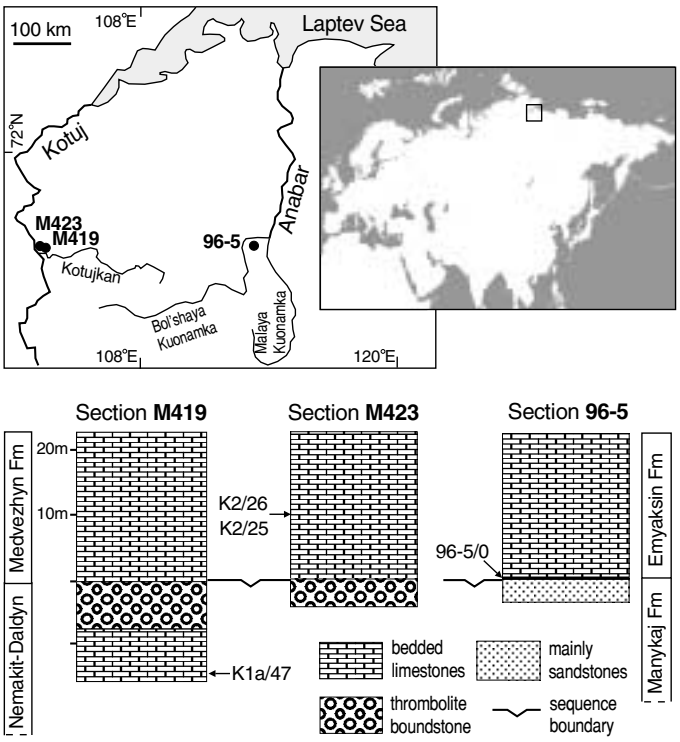

Fig. 1. Location maps and generalized stratigraphic columns showing sampling localities and levels for the described material.

Material and methods

The material was collected during two expeditions to the Anabar Uplift, Siberian Platform (Fig. 1): to the Kotuj River in 1992 (participants AK and Pyotr Yu. Petrov) and to the Malaya and Bol'shaya Kuonamka Rivers in 1996 (participants AK, SB, Anatolij V. Valkov, Vladimir V. Missarzhevsky and Shane Pelechaty). Section M423 (Rozanov et al. 1969) is situated at the mouth of the Kugda brook on the right bank of the Kotuj River. From a 25–30 m thick succession of richly fossiliferous normal marine carbonates of the Medvezhin Formation, 40 samples were collected (by AK) in 1992. The anabaritids preserved in celestite are from samples K2/25 and K2/26 from the uppermost part of a 1.2 m thick wackestone bank distinguished by its lighter colour in the lower part of the outcrop. Numerous dissolution surfaces occur throughout the unit, and diabase dykes, about 1 m thick and tens of meters apart, cut the entire section. Visible zones of hot contact with the carbonates extend up to several decimetres. Section M419 (Rozanov et al. 1969), situated ca. 2 km upstream of the mouth on the right bank of the Kotujkan, represents the Nemakit-Daldyn Formation; Sample K1a/47 was collected (in 1992, by AK) from the lower part of unit 11 (Rozanov et al. 1969) and is a wackestone from the vicinity of an algal build-up. Section 96-5 (A-50 of Val'kov 1975) is by the Bol'shaya Kuonamka River, at the mouth of a small creek that feeds from the left into the Ulakhan-Tjulen brook about 1 km from its mouth. The sample 96-5/0 from the base of the Emyaksin Formation is a coarse sandstone with calcareous cement.

The fossils represent tubes of anabaritids replaced by celestite and barite, and phosphatic internal moulds of tubes with replicated microstructures. They were extracted from the samples with dilute acetic acid. Pictures were taken with scanning electron microscopes (SEMs; Philips XL-30 and Hitachi S4300). Thin sections were coated with carbon and investigated with energy-dispersive spectrometers (EDS) at-

Fig. 2. *Jacutiochrea tristicha* (Missarzhevsky), specimen SMNH X3409 (same as in Figs. 5 and 3), sample K2/25. **A**. Fractured section through a flange and wall. **B**. Septum-like protrusion of the tube wall surrounded by apatitic internal mould (note flattened surface of apatite layer). **C**. Tube with transverse flanges (arrows correspond to close-ups shown in A, B, D–J). **D**. Bundle arrangement of fibres in the wall. **E**. Close-up of D (arrowed) with minute fibres at boundary between adjacent bundles. **F**. Close-up of G, with different inclination of fibres in adjacent lamellae. **G**. Transition of wall into flange, and bilamellar construction of the wall at the flange. **H**. 45° inclination of fibres in a flange (note the phosphatic crust embedding the flange). **I**. Arrangement of fibres in a broken flange. **J**. Flange consisting of radially oriented inclined fibres and covered with a thin phosphatic crust. →

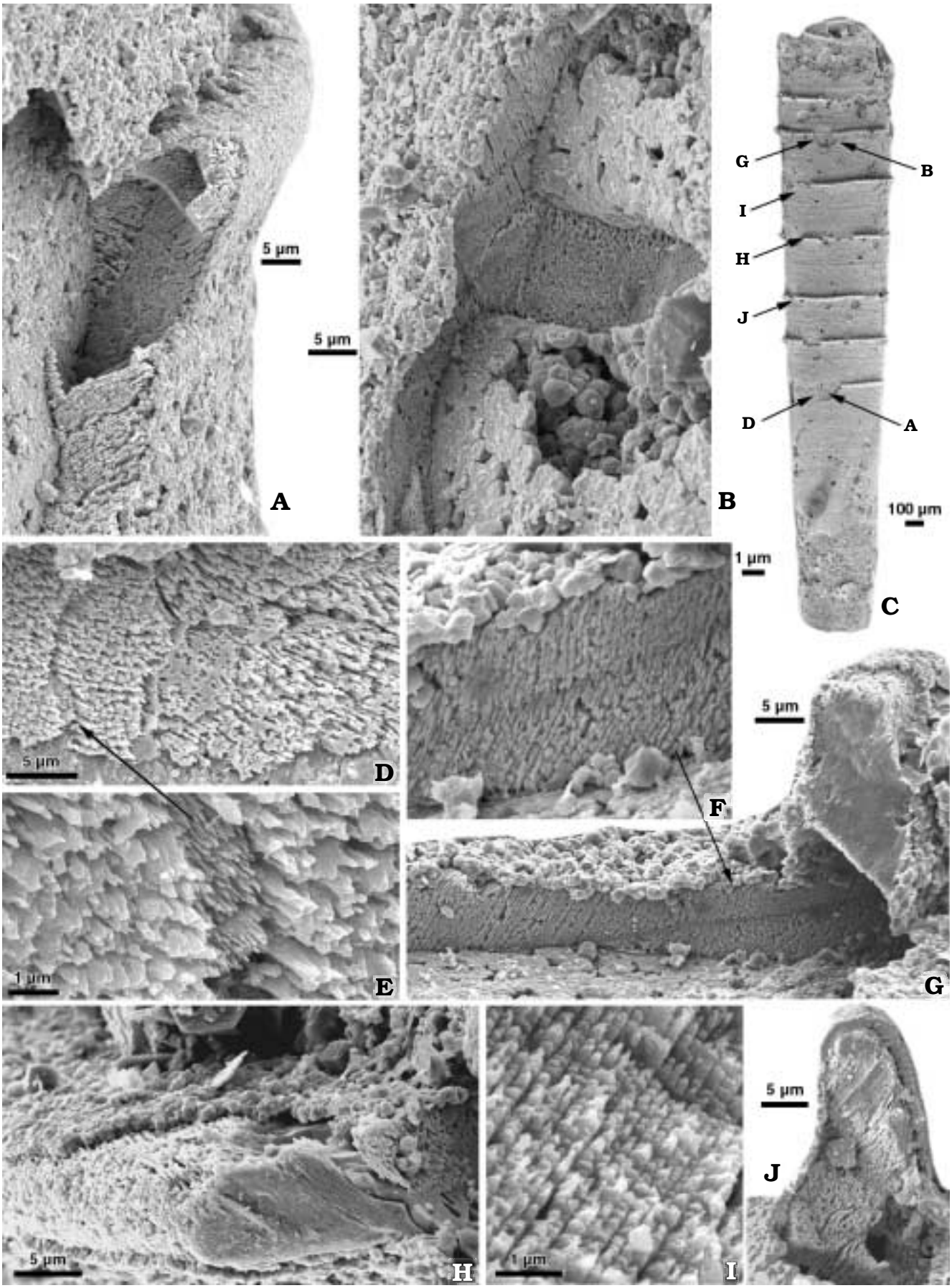
5 µm
A
5 µm
B
G
B
I
H
J
D
A
100 µm
C
1 µm
5 µm
D
F
5 µm
1 µm
E
G
5 µm
H
1 µm
I
5 µm
J

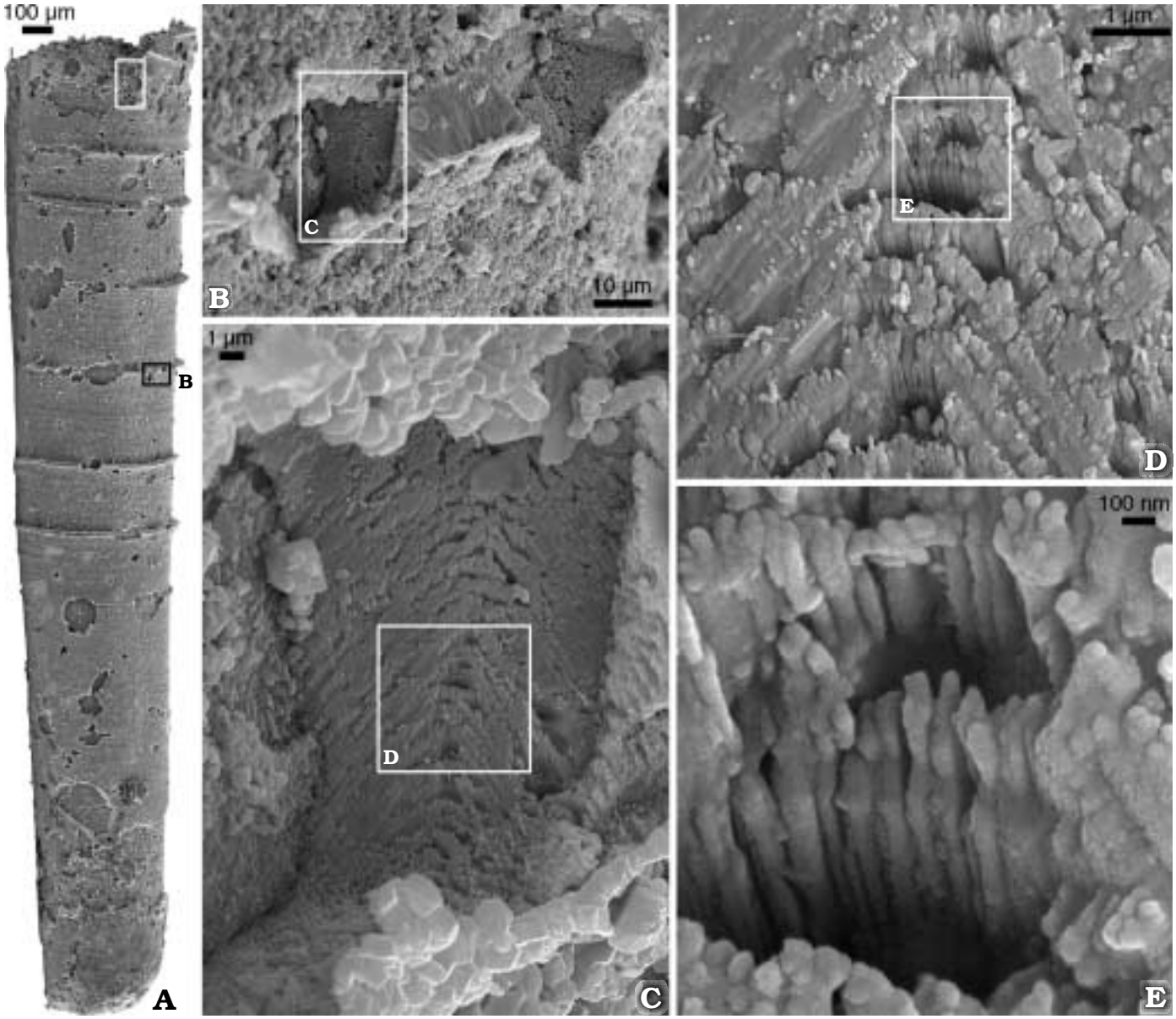

Fig. 3. *Jacutiochrea tristicha* (Missarzhevsky), specimen SMNH X3409 (same as in Figs. 2 and 5), sample K2/25. **A**. Tube, with positions of B and of Fig. 5A indicated. **B**. Close-up of A, showing position of chevron pattern in relation to flange. **C**. Close-up of B, showing chevron pattern. **D**. Close-up of C, showing detail of chevron pattern and fibre-shaped elements. **E**. Close-up of D, showing fibres. Rounded tips of fibres and fine granulosity are features of the gold coating.

tached to the respective SEMs. Powder X-Ray Diffraction analyses were carried out with a Philips PW 1830.

All the material is deposited in the Museum of Natural History, Stockholm, Sweden, abbreviated SMNH, under the numbers X3409–3415, X3516–3517.

Celestite-preserved anabaritids

The walls of *Jacutiochrea tristicha*, *Tiksitheca* cf. *licis*, and *Cambrotubulus conicus* analysed with EDS consist mainly of mineral aggregates containing Sr, Ba, S, and O. The Sr:Ba ratio (in atomic percentages) varies from 50:50 to 72:28. The atom content of S is close to the combined content of Sr and Ba, but may differ from it by up to 25%. Powder XRD analysis confirms the mineral phases to be celestite ($SrSO_4$) and barite ($BaSO_4$), which may co-precipitate. As Sr^{2+} is the dominating cation, for simplicity we will refer to the mineral as celestite. The higher sulphur content in places may be due to the presence of pyrite and gypsum, as indicated by traces of Ca and Fe. The lower sulphur content may be the result of the presence of some Sr and Ba ions in the crystalline lattice of calcium carbonate or phosphate.

Jacutiochrea tristicha (Missarzhevsky, 1969 in Rozanov et al. 1969) is represented by two 3 mm long, straight thecal fragment (Figs. 2C, 3A, 4A) and numerous phosphatic inter-

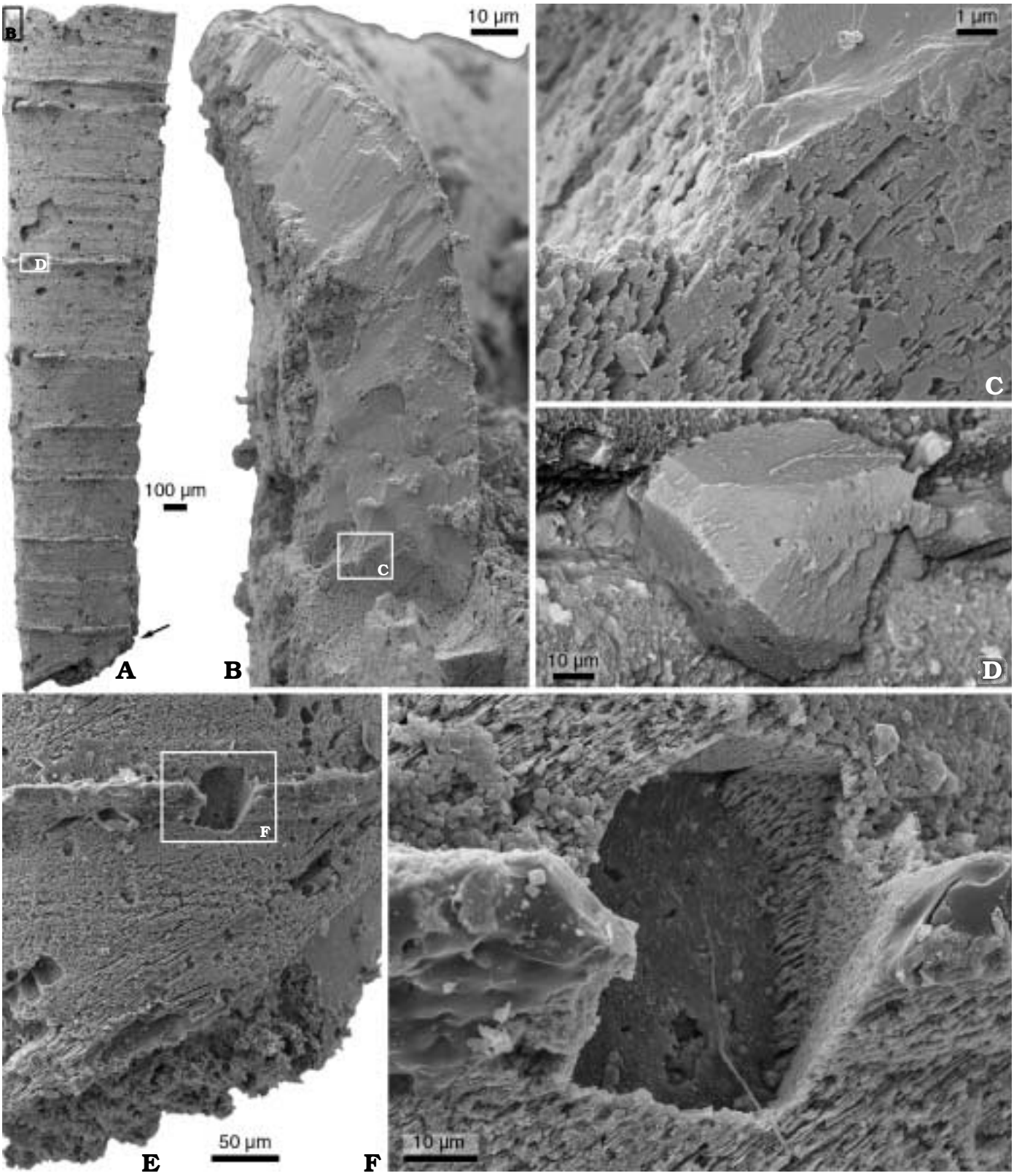

Fig. 4. *Jacutiochrea tristicha* (Missarzhevsky), specimen SMNH X3416, sample K2/25. **A**. Tube, with positions of B, D and E (arrow) indicated. **B**. Close-up of A, showing fractured apertural flange. **C**. Close-up of B, showing boundary between inner, fibrous, and outer, more solid, fabric. **D**. Close-up of A, showing hole after euhedral crystal penetrating the celestite-replaced wall. Picture light-dark inverted to make crystal habit more visible. **E**. Close-up of lower part of tube (slightly tilted from A), showing persistent celestite cleavage pattern oblique to axis of tube. **F**. Close-up of E, showing hole after euhedral crystal and celestite cleavage pattern.

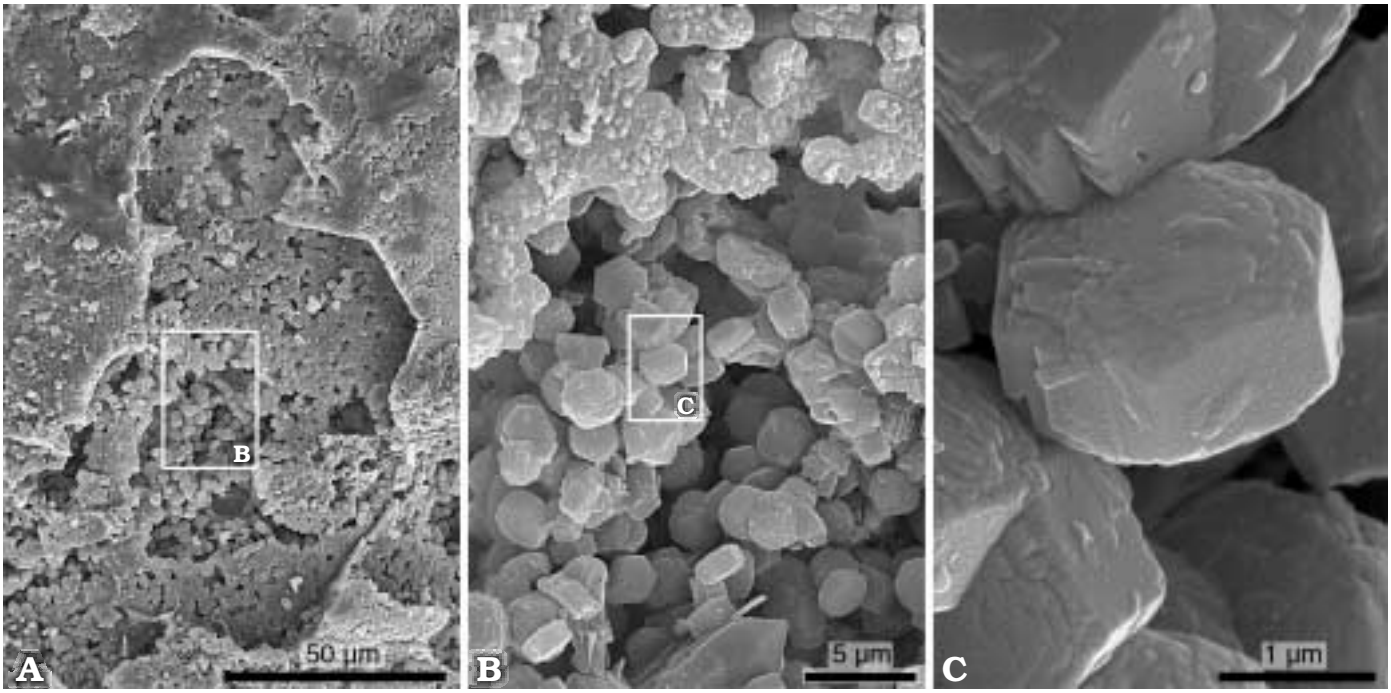

Fig. 5. *Jacutiochrea tristicha* (Missarzhevsky), specimen SMNH X3409 (same as in Figs. 2 and 3), sample K2/25. **A**. Close-up of area marked in Fig. 3A, showing apatite encrusting the internal surface of the tube (wall missing in figured window). **B**. Close-up of A, showing hexagonal apatite tablets. **C**. Close-up of B, showing individual tablet.

nal moulds. The cross-sections are rounded hexagonal in the wider part and rounded triangular at the narrow end. The apexes and apertures are not preserved. In the specimen in Figs. 2 and 3, the wall possesses annular flanges 20–30 µm high and 100–250 µm apart, except in the narrower parts of the tube (diameter below 470 µm) where the flanges are absent. Between the flanges, weaker annular rugae are present. The wall thickness is 10–15 µm. At the first and sixth flanges there are tooth-like internal protrusions of the wall. The partially preserved tooth in Fig. 2B is 10–15 µm wide and 20–25 µm long. The specimen in Fig. 4 has a similar flange pattern but does not preserve any narrower portion without flanges; it also has somewhat more pronounced rugae between the flanges.

The walls in the two specimens are celestite-replaced, but the nature of the replacement is somewhat different. The specimen in Fig. 4 shows more of the crystalline structure of the replacing mineral, whereas the one shown in Figs. 2, 3 and 5 appears to preserve the original structure to a greater extent. Comparisons are, therefore, instructive to help distinguish between original and diagenetic microstructure.

Both specimens are coated internally and externally with a layer of apatite. In contrast to the usual type of diagenetic encrustation of apatite on fossils in carbonate rocks (see e.g., Yue and Bengtson 1999: fig. 9), these layers do not consist of fibronormal crystals (needle-shaped, growing perpendicular to encrusted surface) with spherulitic growth pattern. Instead they occur as equidimensional, almost perfect hexagonal apatite tablets, 2–2.5 µm in diameter and about 0.5 µm thick (Fig. 5). Such a crystal habit may derive from dehydration of amorphous collophane or francolite at burial depths of 0.5–1 km (Yermolaev et al. 1999). The outer boundary of the inner apatite layer adjacent to the wall is flattened (Figs. 2B, G, 5A). The outer apatite coating forms a crust a few micrometers thick (Fig. 2G, H, J).

In addition to the apatite coating, the specimens also show imprints of euhedral crystals penetrating the wall from the outside. This is particularly the case with the specimen showing less of the original fabric (Fig. 4D, F). A prevalent striation pattern forming an oblique angle of about 30° to the growth lines can be seen over most of the tube surface (e.g., Fig. 4E). The pattern is continuous with a fine-bladed internal fabric consisting of thin sheets about 0.25–1 µm apart (Fig. 4F). Celestite has a perfect cleavage in the {001} direc-

Fig. 6. *Tiksitheca* cf. *licis* Missarzhevsky, specimen SMNH X3410, sample K2/26. **A**. Tube with prominent concentric flanges and smooth transverse folds between them. **B**. External surface of the tube arrowed at D, partially covered with a phosphatic crust (lower left). **C**. Close-up of B showing outer terminations of fibres. **D**. Tube inside a phosphatic internal mould of a bigger tube. **E**. Phosphatic replica of the lower outer surface of a flange with radial marks of fibres (note a piece of recrystallised wall at the top). **F**. Broken margin of a flange arrowed in B, with outer terminations of fibres (arrow points to phosphatic crust). **G**. Close-up of casts of fibres arrowed in E. **H**. Partially recrystallized wall with fibres fused along their faces, and dissolution cavities that possibly contained calcite before the sample was chemically prepared. **I**. Fractured wall likely displaying recrystallised portions where faces of at least two celestite crystals appear (arrowed). →

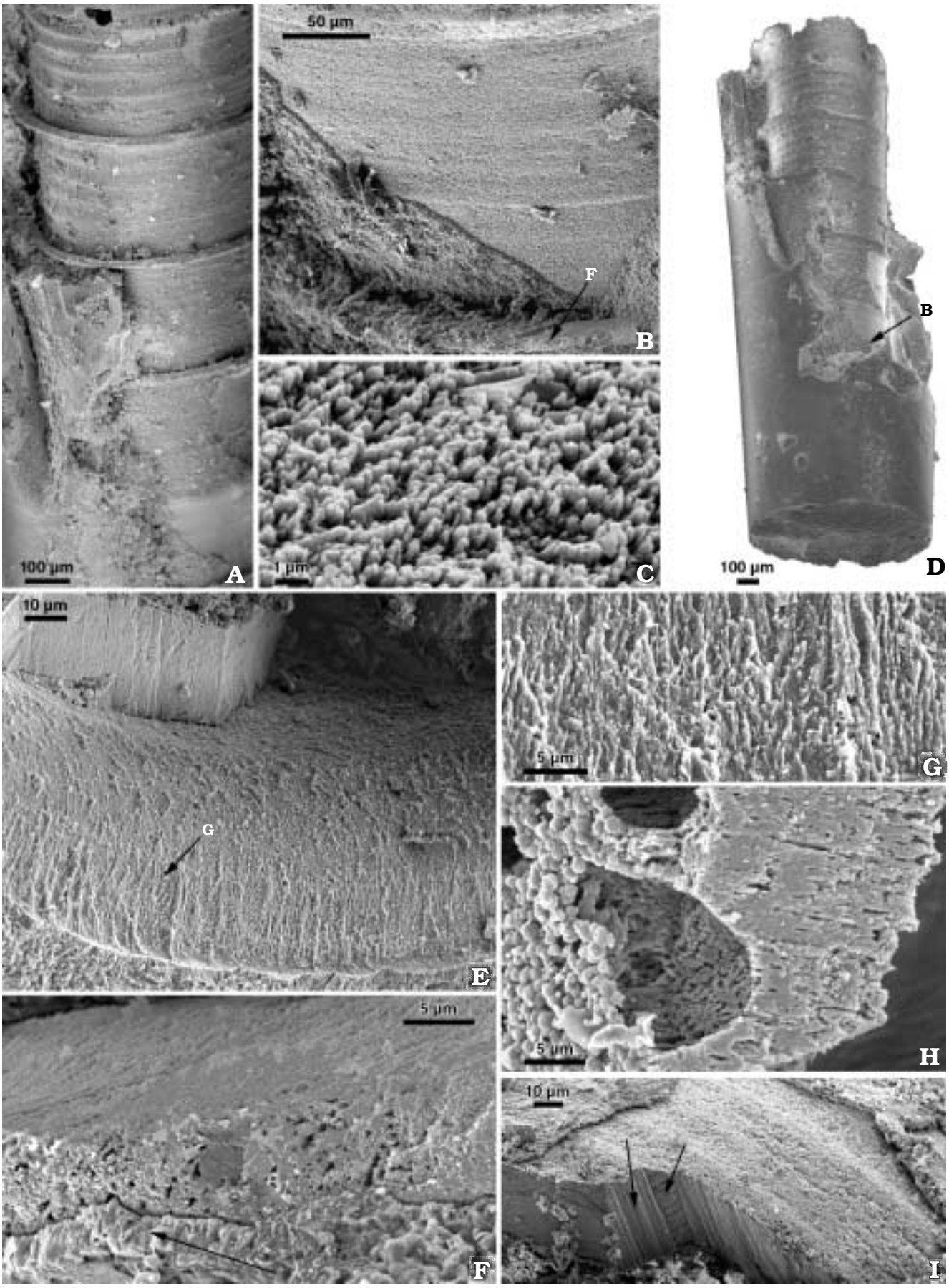
100 µm
A
50 µm
F
B
1 µm
C
B
100 µm
D
10 µm
G
E
5 µm
G
5 µm
H
5 µm
F
10 µm
I

tion. We interpret the oblique striation and bladed fabric to reflect this cleavage; the constant direction suggests that the wall of the whole specimen has been replaced by one celestite crystal.

The other specimen of *Jacutiochrea tristicha* (Figs. 2, 3) shows a number of structures which, although sometimes similar to the diagenetic structures described above, are clearly related to the original structure of the shell wall. Fractures through the wall near a flange reveal a conspicuous chevron-like structure, where 0.2–0.3 μm thick laminae of parallel fibres form V-shaped structures with their rounded tips pointing in the direction of the aperture (Fig. 3). The layers are clearly continuous over the tips of the Vs (Fig. 3D, E), indicating that the structure was not formed by the coincident boundaries of two celestite crystals but represent recurved laminae.

Other structures in this specimen are more difficult to interpret, because of the interplay between original features and celestite replacement. At a number of places, there are boundaries between units having different directions of bladed or fibrous fabrics. Most of these appear to have no direct relationship with tube morphology and could easily be explained as merely representing boundaries between celestite crystals. The bladed fabric in these cases would then likely reflect celestite cleavage rather than original wall structure. Some recurring patterns may, however, represent original structures. One such pattern seems to be related to the accretion of the tubes near the flanges: in these cases the boundaries between the units are in the vicinity of flanges and form an oblique angle of about 30° with the inner surface of the wall (Fig. 2A, F, G). It is known from other replaced shell fabrics (Maliva and Dickson 1992) that the boundaries of replacing crystals sometimes trace the boundaries of the original growth lamellae. The oblique crystal boundaries in *J. tristicha* may thus reflect surfaces where original lamination has defined the boundaries of replacing celestite crystals. Whether the original structure was formed by growth lamination (for example, by a wedge-formed beginning of new tube growth following the formation of a flange) or by other structures (for example, the track of consecutive tips in the chevron-shaped growth lamination shown in Fig. 3) cannot presently be determined.

In other sections of the tube, the wall lamellae consist of inclined parallel fibres around 0.2 μm thick (Fig. 2D, E). In some places the fibres are arranged in 5–15 μm wide bundles. The boundaries between adjacent bundles are 1 μm wide and consist of parallel thinner fibres, 0.1 μm thick (Fig. 2E). These structures also appear to have a biological, rather than diagenetic, origin. The outer portions of the flanges tend to present cleaner fracture surfaces, with less pronounced bladed or fibrous structures than in the inner parts of the tubes (Figs. 2H, G, J, 4B, C).

Tiksitheca cf. *licis* Missarzhevsky, 1969 (in Rozanov et al. 1969), is represented by a 3 mm long thecal fragment with a rounded triangular cross section. It is preserved in celestite inside the phosphatic internal mould of a separate and larger tube (Fig. 6D). The wall has six prominent annular flanges, 30–50 μm high and 300 μm apart (Fig. 6A, D), intercalated with low, smooth rugae parallel to the flanges (Fig. 6A). Each flange consists of subradially oriented fibres, up to 0.3 μm in diameter (Fig. 6E–G). The same fibres appear at the outer surface of the tube (Fig. 6B, C) and at a broken flange (Fig. 6F). The wall is 20–35 μm thick. In some places a fractured wall displays dissolution cavities (Fig. 6H) or blocky celestite crystals (Fig. 6I). Most of the tube is covered with a thin phosphatic crust (Fig. 6B, F).

Fracturing the wall of this specimen (Fig. 7) reveals a structure closely similar to that observed in *Jacutiochrea tristicha* (Fig. 3). The wall inside the flanges has a distinct chevron pattern, formed by recurved laminae with the convexity pointing toward the aperture (Fig. 7B). Further away from the flanges the same laminae have an oblique and more-or-less sinuous course (Fig. 7C–E), but typically forming an angle with the tube wall of at least 45°; in some cases the distinction between original lamination and celestite cleavage may be difficult to discern (e.g., Fig. 7D).

Cambrotubulus conicus Missarzhevsky, 1989, is available as a tube without the initial part, but with the preserved aperture (Fig. 8B–C). The tube is 2 mm long, circular in cross section (Fig. 8D), and composed of longitudinally oriented fibres of celestite, possibly arranged in bundles (Fig. 8A). Delicate growth lines cover the surface of the tube (Fig. 8C, D).

Phosphate-preserved anabaritids

The specimen of *Anabarites tricarinatus* Missarzhevsky, 1969, is preserved as a phosphatic cast of the outer thecal surface, with growth lines curved towards the aperture and replicated fibres about 2 μm wide (Fig. 9A, B). The species has a star-shaped cross-section (Rozanov et al. 1969; Abaimova 1978). Each of its three lobes ends in a prominent undulating longitudinal keel with casts of fibres almost perpendicular to the longitudinal axis of the tube (Fig. 9G). The fibres on the lobes are oriented perpendicularly to the growth lines following their curvature (Fig. 9F).

Anabarites modestus Bokova, 1985, is represented by an almost straight phosphatic internal mould, 1 mm long, with a rounded triangular cross-section (Fig. 9H). The fossil derives from the type locality of *A. modestus* Bokova (Bokova 1985). There are remains of a smooth phosphatic crust in some places of the mould (Fig. 9I). The crust probably covered the outer surface of the now dissolved tube. The thickness of the wall is 5–10 μm. There are longitudinally oriented, parallel or slightly diverging casts of fibres and transverse growth marks. The thickness of the fibres is around 1 μm. In places they are arranged in a fan-like manner (Fig. 9J). The fan-like pattern may have resulted from replication of fibrous aggregates having spherulitic growth and a low angle of inclination of the fibres to the thecal surface. The structures resemble the inner layer with spherulitic structure reported from in-

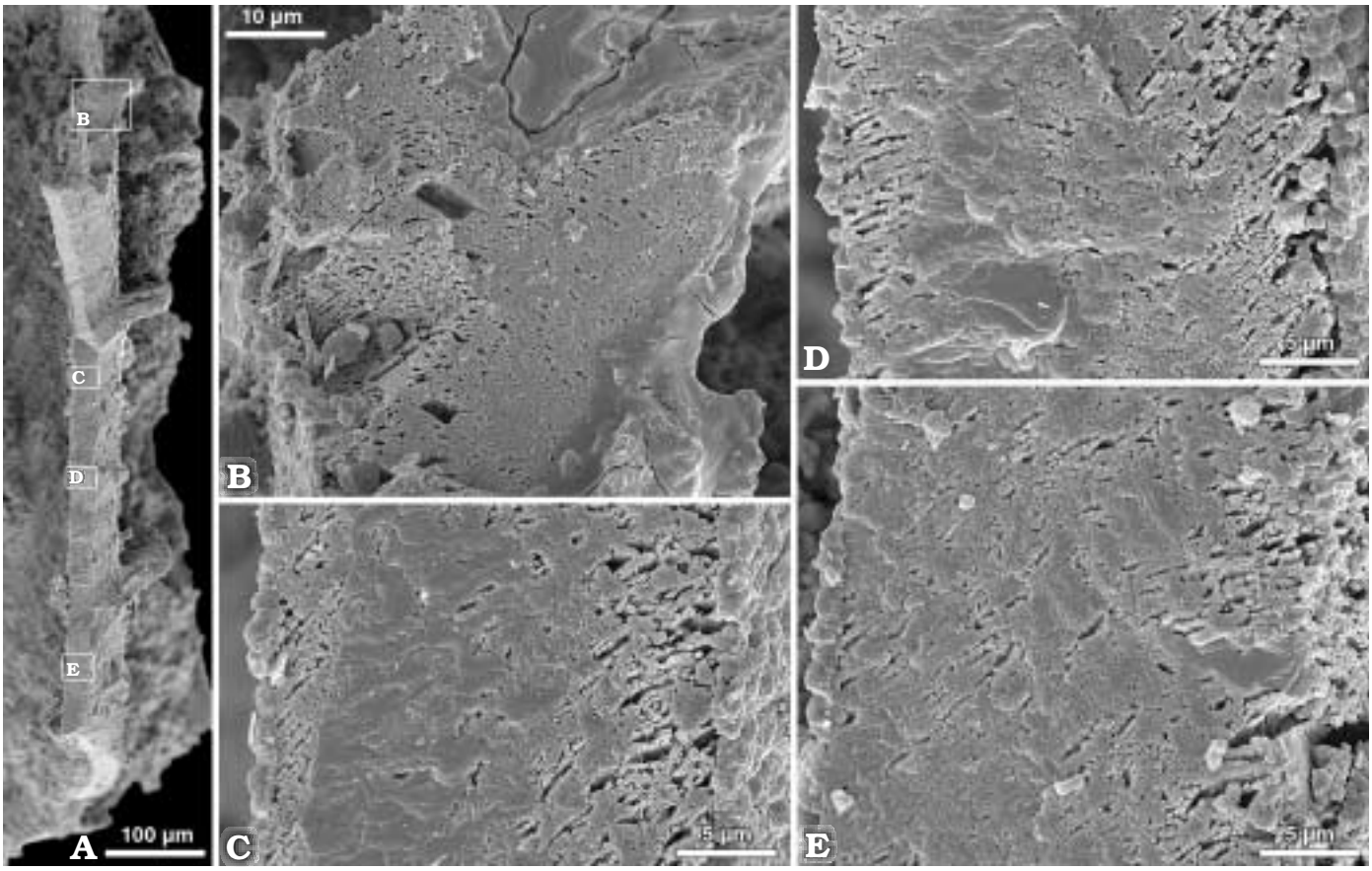

Fig. 7. *Tiksitheca* cf. *licis* Missarzhevsky, specimen SMNH X3410, same as in Fig. 6 after inner tube has been broken longitudinally to expose internal wall structure. **A**. Tube wall, with positions of B–E indicated. **B**. Close-up of A, showing chevron pattern inside flange and curved laminae within flange (cf. Fig. 11). **C**–**E**. Close-ups of A, showing oblique and partly sinuous growth laminae in non-flanged portions of the wall.

ternal moulds of *Anabarites rotundus* Qian, 1977, from China (Conway Morris and Chen 1989).

Anabarites cf. *signatus* Mambetov, 1981 (in Missarzhevskij and Mambetov 1981), is represented by a curved phosphatic internal mould, about 1 mm long, divided into three lobes by narrow grooves (Fig. 9D). A phosphatic crust covered the outer surface of the tube. Remains of the crust are preserved on the mould and reflect three narrow grooves twisted anti-clockwise at about 90° (Fig. 9C). The thickness of the wall was about 10 µm. Casts of fibres are 1–2 µm thick; the same fibres are replaced by phosphate below the crust (Fig. 9B, C). They are arranged longitudinally and subparallel to the tube surface. Some of them diverge from a longitudinal line or a centre (Fig. 9B). Other specimens from the same sample do not show any casts of fibres on the surface of the internal moulds (Fig. 9E).

Preservation of structure during recrystallization

The most studied system of mineral replacement involving preservation of original structures in fossils is the conversion of aragonite to its polymorph calcite or to other minerals. These have been subject to laboratory experiments as well as field studies and application of theoretical diffusion models (e.g., Dodd 1966; Land 1967; James 1974; Maliva and Siever 1988; Maliva and Dickson 1992; Maliva 1998). Aragonite is metastable under normal marine conditions. Extrapolations from laboratory measurements under higher temperatures suggest that at 25°C in water, aragonite inverts spontaneously to the more stable calcite in about 10^7 years (Land 1967). This is only a crude estimate, however; longer as well as shorter actual inversion times are known from the fossil record.

Most commonly, the aragonite is simply dissolved as the result of pore-water undersaturation. This usually leads to a destruction of the shell, resulting in a strong preservational bias against aragonitic shells (Cherns and Wright 2000). If the dissolved aragonite instead leaves a void or is replaced by an authigenic mineral, such as calcite, the original aragonitic composition may be inferred if calcitic skeletons in the same beds are preserved with their original fabric (e.g., James and Klappa 1983). When direct inversion takes place, however, the original aragonitic fabric may be partly preserved in the resulting authigenic calcite (e.g., Land 1967; Carter 1990a, b). Recrystallization in this case takes place along a moving solution front that appears to be driven by the stresses result-

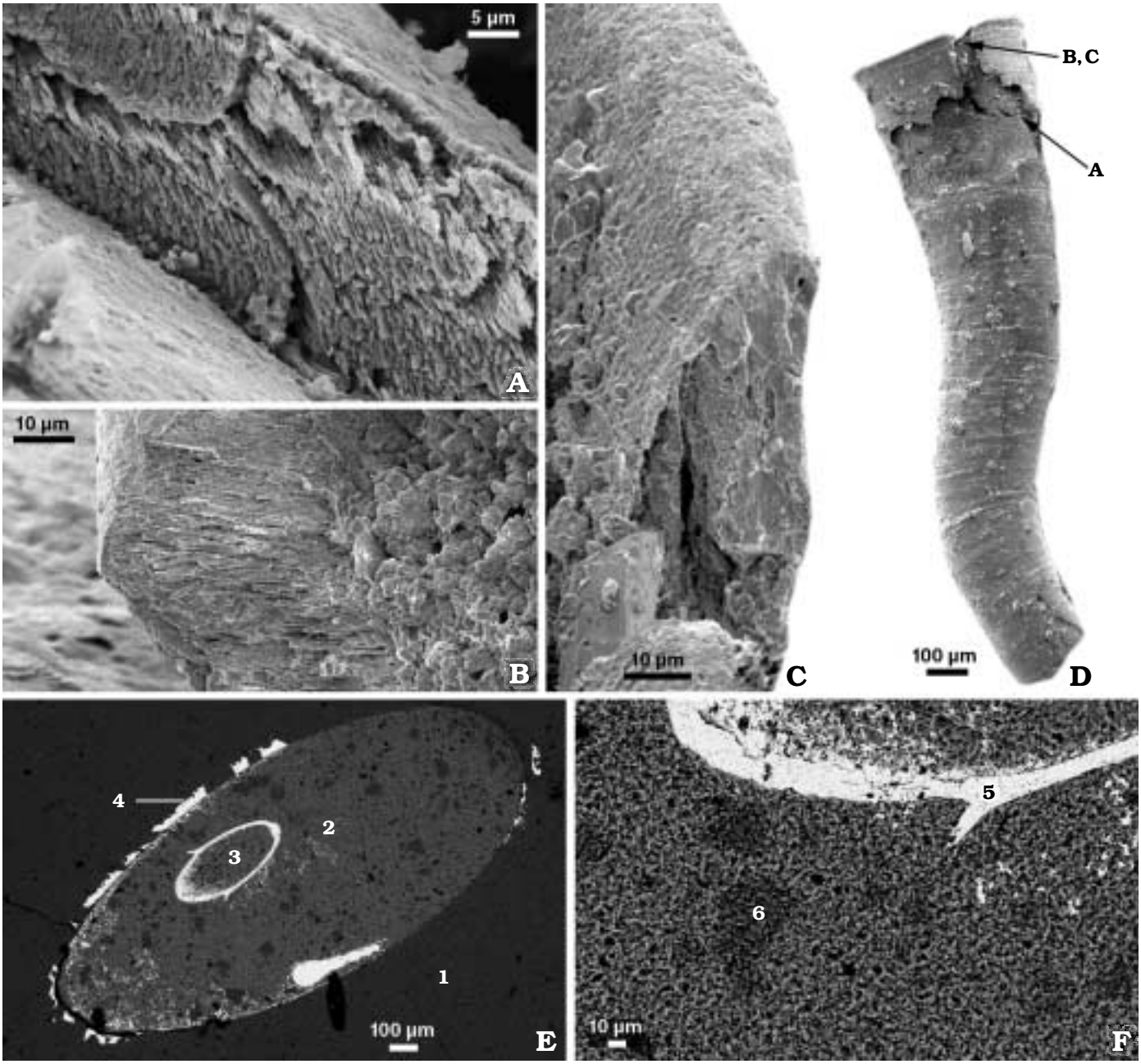

Fig. 8. **A**–**D**. *Cambrotubulus conicus* Missarzhevsky, specimen SMNH X3411, sample K2/25. **A**. Broken wall with fibres arranged in bundles (?) and covered with a diagenetic phosphatic crust. **B**, **C**. Apertural lip with fibres below phosphatic crust. **D**. General view of the tube with growth lines and aperture (the arrows correspond to close-ups in A–C). **E**. Polished section of sample K2/26; back-scattered electron image, where brighter areas indicate higher densities. **F**. Close-up of E. Indicated in E and F are: 1, matrix consisting of micritic calcite with low phosphate and argillaceous admixture; 2, matrix of internal mould of a bigger tube similar to matrix in 1, but lighter because of a higher phosphorus content; 3, matrix of internal mould of a smaller tube identical to 2; 4, protuberances of celestite (with barite) representing remains of a larger tube; 5, wall of a smaller tube consisting of celestite (with barite); 6, zone with a higher calcite content, the brightness of which is similar to that of the outside matrix in 1.

ing from the growth of the authigenic crystals (Maliva and Siever 1988). The crystal boundaries of the original aragonite may be preserved as shadows in the replacing crystals (presumably due to organic sheaths enveloping the original crystals), or may even direct the boundaries of the latter; more rarely are the crystallographic axes inherited (Maliva and Dickson 1992).

Aragonite commonly incorporates strontium in its lattice, Sr substituting for Ca. The proportion of Sr ions to total Ca positions in naturally occurring aragonite may be almost 5% (Chang et al. 1996: 238–239), or about 40,000 ppm of dry weight. The Sr content of fossil aragonitic shells typically lies between 1000 and 10,000 ppm; if the solution film along the inversion front is in communication with the pore water,

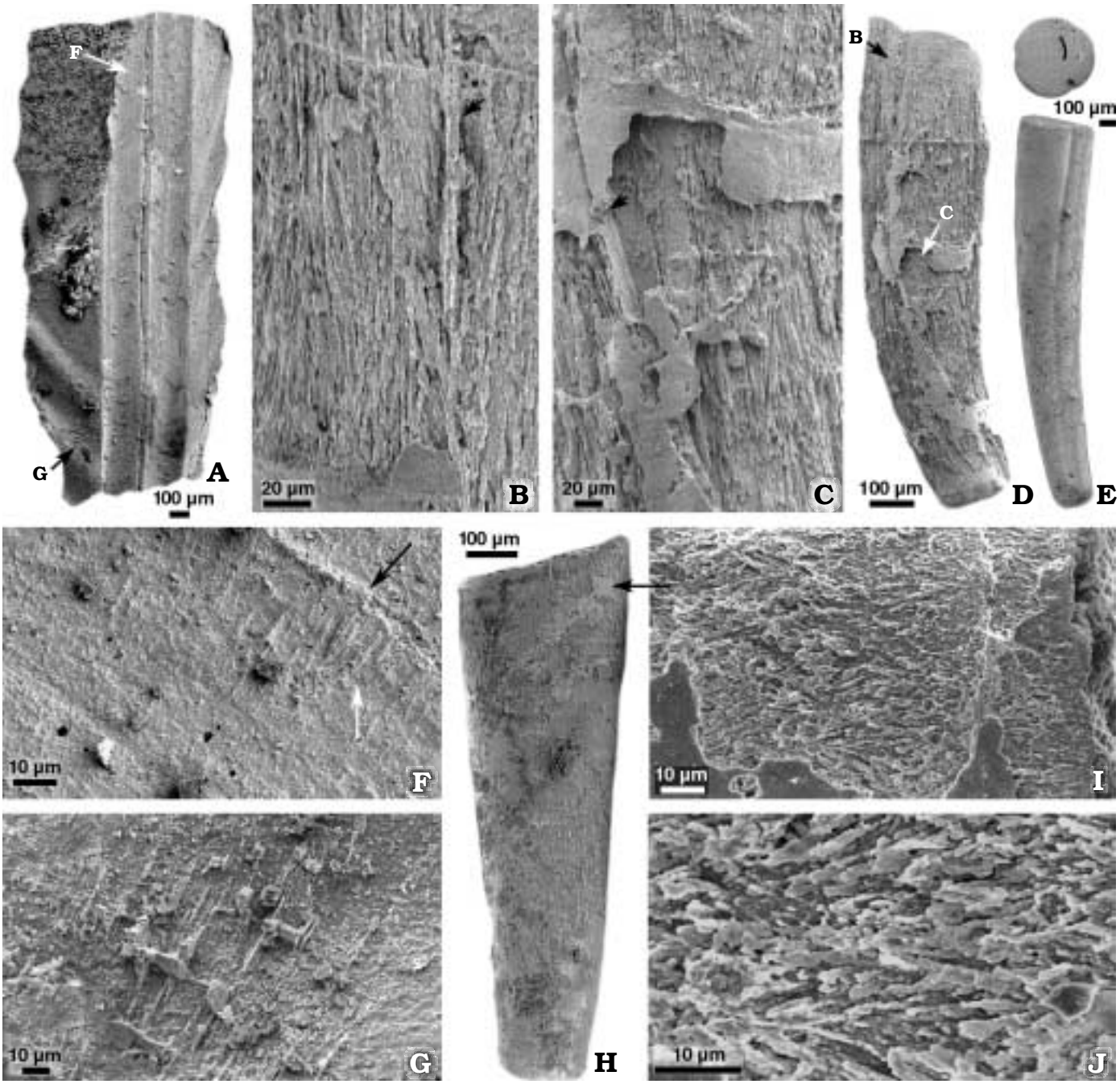

Fig. 9. **A**, **F**, **G**. *Anabarites tricarinatus* Missarzhevsky; specimen SMNH X3412, sample K2/25. **A**. Phosphatic replica of the outer surface, general view; aperture towards top of figure (the arrows correspond to close-ups in F and G). **F**. Casts of fibres (white arrow) perpendicular to growth lines (black arrow) from area indicated in A (aperture toward bottom of picture). **G**. Casts of fibres perpendicularly oriented to the longitudinal axis of the tube from the area of a replicated longitudinal keel indicated in A. **B**–**E**. *Anabarites* cf. *signatus* Mambetov; specimens SMNH X3413 (**B**–**D**), and SMNH X3414 (**E**) from sample 96-5/0. **B**. Close-up of the area at the aperture arrowed in D with phosphatized fibers (?). **C**. Close-up of the area with an attached outer phosphatic crust (arrowed in D) reflecting a longitudinal groove (arrowed). **D**. Overall view of phosphatic internal mould (arrows correspond to close-ups in B and C). **E**. Another internal mould without replicated fibres, but with longitudinal grooves (lower part of the figure), and a cross-section of the specimen (upper part of the figure). **H**–**J**. *Anabarites modestus* Bokova, specimen SMNH X3415, sample K1a/47. **H**. General view of phosphatic internal mould with phosphatic casts of fibres and remains of an outer phosphatic crust. **I**. Longitudinal phosphatic replicas at the aperture and an outer smooth phosphatic crust (lower part of the figure). **J**. Close-up of I showing replicated fibres arranged in a fan-like manner.

generally most of the Sr is lost during the conversion to calcite (Maliva 1998).

Replacement of aragonite by non-polymorphic minerals such as silica or celestite, although they call for considerable exchange with the bulk pore water, tends to be as effective in preserving original textures as aragonite–calcite inversion.

Maliva and Dickson (1992) reported millimeter-sized celestite crystals replacing both micrite and aragonitic grains in Pliocene limestones from the Bahamas, preserving ghosts of original crossed-lamellar mollusc microstructures. This preservation appears to be comparable with what we report here from Cambrian anabaritids.

Interpretation of anabaritid wall structure

The main recognizable building elements of the anabaritid tube wall are long, acicular units forming fibres a few tenths of a micrometer wide. As this is a common crystal habit of aragonite, and anabaritid walls preserved in carbonate always appear to be recrystallized, we concur with previous assessments that the original mineral of the wall was aragonite rather than calcite. The fibres are aggregated into thin laminae, and in *Jacutiochrea tristicha* and *Tiksitheca* cf. *licis* these have been observed to have a direction strongly oblique to the outer and inner tube walls, and to form a conspicuous chevron pattern in connection with the flanges (Fig. 10). In *J. tristicha* and *Cambrotubulus conicus* the fibres may occasionally form bundles of varying dimensions and directions, but the relationship of these bundles to the growth laminae is not clear. They may be related to the spherulite-like structures fanning out in the apertural direction, as observed on the surfaces of phosphatic internal moulds of species of *Anabarites*. The structure of the outer parts of the wall has not been observed in these species; conversely, the celestite-preserved species (*J. tristicha* and *T.* cf. *licis*) with the strongly oblique lamellae do not show a spherulite-like inner layer.

The evidence for accretionary growth (transverse flanges, growth lamellae) implies biomineralization of epithelially secreted tissue. The chevron-like pattern in *J. tristicha* and *T.* cf. *licis* suggests that at least this part of the wall was formed by building on the leading edges, as suggested by Conway Morris and Bengtson (in Bengtson et al. 1990: 197), on the basis of the presence of external longitudinal keels in some anabaritids. This growth may have been accomplished by a localized glandular epithelium similar to the collar organ of serpulid polychaetes (Hedley 1958; Neff 1971; Clark 1976; Weedon 1994; secretory zone in Fig. 11 herein).

As remarked initially, most authors have interpreted the anabaritids as either of uncertain systematic position or as belonging to the Cnidaria, possibly close to the Scyphozoa. The few exceptions are the original suggestion by Voronova and Missarzhevsky (1969) and the subsequent comment by Glaessner (1976), based on morphological comparisons, that anabaritids may be tubicolous polychaetes, belonging to the Serpulida. The new observations of the anabaritid wall structure are in several ways reminiscent of the structure of serpulid tubes. In particular, this concerns the pattern of growth lamellae bent into chevron shape, which in serpulids

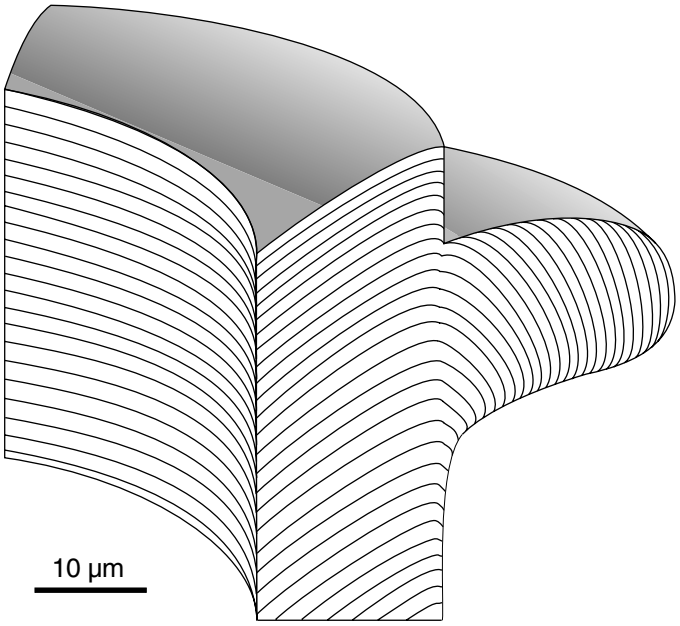

Fig. 10. Reconstruction of growth laminae of *Jacutiochrea tristicha* and *Tiksitheca* cf. *licis* in flanged portion of the wall (cf. Fig. 7B).

is formed by calcium-secreting glands in the collar organ. In addition, Weedon (1994) has described a thin spherulitic layer in the serpulid *Spirorbis*, although this is on the outside of the tube, rather than on the inside as in anabaritids.

Until now, a chevron-like structure of the walls has been considered unique to serpulids (Weedon 1994). The additional presence in both serpulids and anabaritids of a spherulitic layer may seem to be a strong corroboration of the earlier suggestions by Voronova and Missarzhevsky (1969) and Glaessner (1976) that the two groups are related. However, a spherulitic growth pattern is a natural growth habit for aragonite and calcite (as well as a number of other minerals). In inorganic and many organic systems, aragonite commonly displays fibrous habit as well as spherulitic growth. Nucleated at random on a substrate, spherulitic prisms (or bundles) grow competitively to achieve more or less uniform shape following the rule of soap-bubble geometry (Runnegar 1989). Spherulites are therefore a common pattern in shell ultrastructure, particularly in organisms with limited ability to control the crystal shape, such as corals (Constantz 1986). It signifies lack of biological control rather than indicating a specific biomineralization mechanism with phylogenetic significance. Nonetheless, a number of shell-bearing animals do not show such a pattern (although it is common in cnidarians, otherwise the prime candidate for anabaritid affinity).

Anabaritids frequently have internal tooth-like projections (e.g., Fig. 2B) that would have hampered the up-and-down movements in the tubes that characterize serpulids. As pointed out by Weedon (1994: 6), the serpulid tube is "a protective dwelling place for the animal rather than an integral skeletal part of the animal itself". Nonetheless, *Pomatoceros* is known to be able to repair the posterior end of its tube with

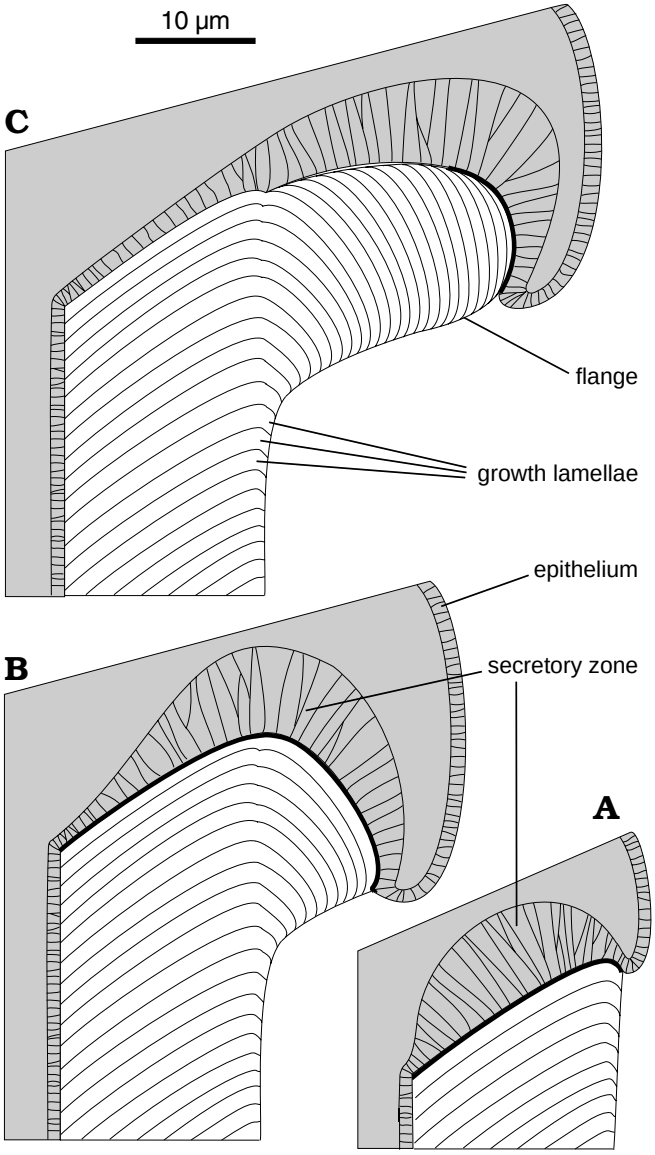

Fig. 11. Interpretative drawing of section through *Jacutiochrea tristicha* and *Tiksitheca* cf. *licis*, showing relationship between tube wall (white) and soft tissues (grey) during normal tube growth (**A**) and flange formation (**B**, **C**). Thick black line indicates growing edge of tube wall.

a septum-like calcareous structure secreted by the hind end of the body (Hedley 1958). Thus serpulids do at least seem to have the ability to form internal tube structures to some extent restricting movement.

There may be a considerable stratigraphic gap between anabaritids and indubitable serpulids. Weedon (1990; 1991) demonstrated that Palaeozoic fossils traditionally assigned to serpulids in fact lack the chevron lamellae and represent a secretory mode more similar to that of brachiopods, bryozoans, and molluscs; serpulids may thus not have appeared until the Mesozoic (Weedon 1994). Irrespective of interpretations of anabaritid affinity, however, the new evidence shows that the main shell-forming tissue of anabaritids was localized to a ring-shaped zone by the tube aperture. Thus there seems not to have been an extended secreting epithelium like the mantle in mollusc or basal epithelium in cnidarians. Kouchinsky et al. (1999) discovered probable cnidarian embryos associated in Early Cambrian deposits on the Siberian Platform and speculated that these may in fact belong to the co-occurring anabaritids. Whereas this possibility still remains, it would be negated by the acceptance of the here described anabaritid wall structure as evidence for serpulid affinity.

Acknowledgements

We thank Pyotr Yu. Petrov, Anatolij V. Valkov, Vladimir V. Missarzhevsky and Shane Pelechaty for companionship and help in the field. Simon Conway Morris gave helpful criticism on an earlier version of the manuscript, and he and Joseph Carter reviewed the submitted manuscript. Elena V. Tolmacheva and Raisa P. Kotina gave some mineralogical advice. Our work has been financially supported by grants from the Royal Swedish Academy of Sciences (KVA) and the Swedish Natural Science Research Council (NFR).

References

Abaimova, G.P. 1978. Anabaritids – ancient fossils with carbonate skeleton [In Russian]. *Trudy SNIIGGIMSa* 260: 77–83.

Bengtson, S. 1994. The advent of animal skeletons. *In*: S. Bengtson (ed.), *Early Life on Earth. Nobel Symposium 84*, 412–425. Columbia University Press, New York, N.Y.

Bengtson, S., Conway Morris, S., Cooper, B.J., Jell, P.A., and Runnegar, B.N. 1990. Early Cambrian fossils from South Australia. *Memoirs of the Association of Australasian Palaeontologists* 9: 1–364.

Bokova, A.R. 1985. The oldest complex of organisms in the Cambrian of the western Anabar region [in Russian]. *In*: V.V. Khomentovskij, A.A. Terleev, and S.S. Bragin (eds.), *Stratigrafiâ pozdnego dokembriâ i rannego kembriâ paleozoâ Sibiri*, 13–28. Institut Geologii i Geofiziki SO AN SSSR, Novosibirsk.

Carter, J.G. (ed.) 1990a. *Skeletal Biomineralization: Patterns, Processes and Evolutionary Trends*, vol. 1. 832 pp. Van Nostrand Reinhold, New York, N.Y.

Carter, J.G. (ed.) 1990b. *Skeletal Biomineralization: Patterns, Processes and Evolutionary Trends*, vol. 2. 101 pp. Van Nostrand Reinhold, New York, N.Y.

Chang, L.L.Y., Howe, R.A., and Zussman, J. 1996. *Non-silicates: Sulphates, Carbonates, Phosphates, Halides*. 383 pp. Longman, Harlow, Essex.

Cherns, L. and Wright, V.P. 2000. Missing molluscs as evidence of large-scale, early skeletal aragonite dissolution in a Silurian sea. *Geology* 28: 791–794.

Clark, G.R., II 1976. Shell growth in the marine environment: approaches to the problem of marginal calcification. *American Zoologist* 16: 617–626.

Constantz, B.R. 1986. Coral skeleton construction: a physiochemically dominated process. *Palaios* 1: 152–157.

Conway Morris, S. and Chen M. 1989. Lower Cambrian anabaritids from South China. *Geological Magazine* 126: 615–632.

Dodd, J.R. 1966. Processes of conversion from aragonite to calcite with examples from the Cretaceous of Texas. *Journal of Sedimentary Petrology* 36: 733–741.

Fedonkin, M.A. 1986. Precambrian problematic animals: Their body plan and phylogeny. *In*: A. Hoffman and M.H. Nitecki (eds.), *Problematic Fossil Taxa*, 59–67. Oxford U.P., New York, N.Y.

Fedonkin, M.A. 1987. The non-skeletal fauna of the Vendian and its place in the evolution of the Metazoa [in Russian]. *Trudy Paleontologičeskogo Instituta AN SSSR* 226: 1–174.

Glaessner, M.F. 1976. Early Phanerozoic annelid worms and their geological and biological significance. *Journal of the Geological Society of London* 132: 259–275.

Hedley, R.H. 1958. Tube formation by *Pomatoceros triqueter* (Polychaeta). *Journal of the Marine Biological Association of the United Kingdom* 37: 315–322.

James, N.P. 1974. Diagenesis of scleractinian corals in the subaerial vadose environment. *Journal of Paleontology* 48: 785–799.

James, N.P. and Klappa, C.F. 1983. Petrogenesis of Early Cambrian reef limestones, Labrador, Canada. *Journal of Sedimentary Petrology* 53: 1051–1096.

Kirschvink, J.L. and Hagadorn, J.W. 2000. A Grand Unified Theory of biomineralization. *In*: E. Bäuerlein (ed.), *Biomineralization*, 139–150. Wiley-VCH, Weinheim.

Kouchinsky, A., Bengtson, S., and Gershwin, L.-a. 1999. Cnidarian-like embryos associated with the first shelly fossils in Siberia. *Geology* 27 (7): 609–612.

Land, L.S. 1967. Diagenesis of skeletal carbonates. *Journal of Sedimentary Petrology* 37: 914–930.

Lowenstam, H.A. and Margulis, L. 1980. Evolutionary prerequisites for early Phanerozoic calcareous skeletons. *Biosystems* 12: 27–41.

Lowenstam, H.A. and Weiner, S. 1989. *On Biomineralization*. 324 pp. Oxford University Press, New York.

Lucas, J. and Prévôt, L.E. 1991. Phosphates and fossil preservation. *In*: P.A. Allison and D.E.G. Briggs (eds.), *Topics in Geobiology*, vol. 9: *Taphonomy—Releasing the Data Locked in the Fossil Record,* 389–409. Plenum, New York.

Maliva, R.G. 1998. Skeletal aragonite neomorphism—quantitative modelling of a two-water diagenetic system. *Sedimentary Geology* 121 (3–4): 179–190.

Maliva, R.G. and Siever, R. 1988. Diagenetic replacement controlled by force of crystallization. *Geology* 16: 688–691.

Maliva, R.G. and Dickson, J.A.D. 1992. The mechanism of skeletal aragonite neomorphism: evidence from neomorphosed mollusks from the upper Purbeck Formation (Late Jurassic–Early Cretaceous), southern England. *Sedimentary Geology* 76: 221–232.

Matthews, S.C. and Missarzhevsky, V.V. 1975. Small shelly fossils of late Precambrian and early Cambrian age: a review of recent work. *Journal of the Geological Society* 131: 289–304.

Missarzhevskij, V.V. [Missarževskij, V.V.] 1974. New data on the oldest Lower Cambrian fossils of the Siberian Platform [in Russian]. *In*: I.T. Žuravleva and A.Û. Rozanov (eds.), *Biostratigrafiâ i paleontologiâ nižnego kembriâ Evropy i severnoj Azii*, 179–189. Nauka, Moskva.

Missarzhevskij, V.V. [Missarževskij, V.V.] 1989. The oldest skeletal fossils and stratigraphy of the Precambrian–Cambrian boundary beds [in Russian]. *Trudy Geologičeskogo Instituta AN SSSR* 443: 1–237.

Missarzhevskij, V.V. [Missarževskij, V.V.] and Mambetov, A.M. 1981. Stratigraphy and fauna of the Precambrian–Cambrian boundary beds in Malyj Karatau [in Russian]. *Trudy Geologičeskogo Instituta AN SSSR* 326: 1–92.

Neff, J.M. 1971. Ultrastructural studies of the secretion of calcium carbonate by the serpulid polychaete worm, *Pomatoceros caeruleus*. *Zeitschrift für Zellforschung* 120: 160–186.

Qian Y. 1977. Hyolitha and some problematica from the Lower Cambrian Meishucunian Stage in central and southwestern China [in Chinese]. *Acta Palaeontologica Sinica* 16: 255–275.

Rozanov, A.Y., Missarzhevskij, V.V., Volkova, N.A., Voronova, L.G., Krylov, I.N., Keller, B.M., Korolyuk, I.K., Lendzion, K., Michniak, R., Pykhova, N.G., and Sidorov, A.D. 1969. The Tommotian Stage and the problem of the lower boundary of the Cambrian [in Russian]. *Trudy Geologičeskogo Instituta AN SSSR* 206: 1–380.

Runnegar, B. 1985. Shell microstructures of Cambrian molluscs replicated by phosphate. *Alcheringa* 9: 245–257.

Runnegar, B. 1989. The evolution of mineral skeletons. *In*: R.E. Crick (ed.), *Origin, Evolution, and Modern Aspects of Biomineralization in Plants and Animals*, 75–94. Plenum, New York, N.Y.

Towe, K.M., Bengtson, S., Fedonkin, M.A., Hofmann, H.J., Mankiewicz, C., and Runnegar, B. 1992. Described taxa of Proterozoic and selected earliest Cambrian carbonaceous remains, trace and body fossils. *In*: J.W. Schopf and C. Klein (eds.), *The Proterozoic Biosphere: A Multidisciplinary Study*, 953–1054. Cambridge U.P., Cambridge.

Val'kov, A.K. 1975. *Biostratigrafiâ i hiolity kembriâ severo-vostoka Sibirskoj platformy.* 139 pp. Nauka, Moskva.

Val'kov, A.K. 1982. *Biostratigrafiâ nižnego kembriâ vostoka Sibirskoj platformy.* 91 pp. Nauka, Moskva.

Val'kov, A.K. and Sysoev, V.A. 1970. Cambrian angustiochreids from Siberia [in Russian]. *In*: A.K. Bobrov (ed.), *Stratigrafiâ i paleontologiâ proterozoâ i kembriâ vostoka Sibirskoj platformy*, 94–100. Âkutskoe Knižnoe Izdatel'stvo, Âkutsk.

Voronova, L.G. and Missarzhevskij, V.V. 1969. Finds of algae and worm tubes in the Precambrian–Cambrian boundary beds in the northern part of the Siberian Platform [in Russian]. *Doklady AN SSSR* 184 (1): 207–210.

Weedon, M.J. 1990. Shell structure and affinity of vermiform "gastropods". *Lethaia* 23: 297–309.

Weedon, M.J. 1991. Microstructure and affinity of the enigmatic Devonian tubular fossil *Trypanopora*. *Lethaia* 24: 227–234.

Weedon, M.J. 1994. Tube microstructure of Recent and Jurassic serpulid polychaetes and the question of the Palaeozoic 'spirorbids'. *Acta Palaeontologica Polonica* 39: 1–15.

Yermolaev, N.P., Sozinov, N.A., Kotina, R.P., Pashkova, E.A., and Goryachin, N.I. 1999. *Concentration Mechanisms of Noble Metals in Terrigenous–Carbonaceous Deposits*. 124 pp. Scientific World, Moscow.

Yue Z. and Bengtson, S. 1999. Embryonic and post-embryonic development of the Early Cambrian cnidarian *Olivooides*. *Lethaia* 32: 181–195.